Constellation-X spectroscopy x-ray telescope assembly and alignment

William Podgorski, David Content, Paul Glenn, Jason Hair, Robert Petre, et al.

William A. Podgorski, David A. Content, Paul E. Glenn, Jason H. Hair, Robert Petre, Timo T. Saha, Mark L. Schattenburg, Jeff Stewart, William W. Zhang, "Constellation-X spectroscopy x-ray telescope assembly and alignment," Proc. SPIE 4851, X-Ray and Gamma-Ray Telescopes and Instruments for Astronomy, (11 March 2003); doi: 10.1117/12.461328

SPIE.

Event: Astronomical Telescopes and Instrumentation, 2002, Waikoloa, Hawai'i, United States

Constellation-X Spectroscopy X-ray Telescope Assembly and Alignment

Dr. William A. Podgorski (SAO)

Co-authors:
Dr. David Content (NASA/GSFC)
Mr. Paul Glenn(Bauer Assoc.)
Mr. Jason Hair (NASA/GSFC)
Dr. Robert Petre (NASA/GSFC)
Dr. Timo Saha (NASA/GSFC)
Dr. Mark Schattenburg (MIT/CSR)
Mr. Jeffrey Stewart (NASA/GSFC)
Dr. William Zhang (NASA/GSFC)

ABSTRACT

The Constellation-X mission is a follow-on to the current Chandra and XMM missions. It will place in orbit an array of four identical X-ray telescopes that will work in unison, having a substantial increase in effective area, energy resolution, and energy bandpass over current missions. To accomplish these ambitious increases new optics technologies must be exploited. The primary instrument for the mission is the Spectroscopy X-Ray Telescope (SXT), which covers the 0.2 to 10 keV band with a combination of two x-ray detectors: a reflection grating spectrometer (RGS) with CCD readout, and a micro-calorimeter. Mission requirements are an effective area of 15,000 cm^2 near 1.25 keV, 6,000 cm^2 near 6 keV, and a 15 arcsec (HPD) resolution requirement with a goal of 5 arcsec. The Constellation-X SXT uses a segmented design with lightweight replicated optics. A technology development program is being pursued with the intent of demonstrating technical readiness prior to the program new start. Key elements of the program include the replication of the optical elements, assembly and alignment of the optics into a complete mirror assembly and demonstration of production techniques needed for fabrication of multiple units. In this paper we present the development of SXT assembly and alignment techniques and describe recent work and current status on the first of these assemblies, the Optical Assembly Pathfinder, in which precision mechanical techniques and optical metrology are used to assemble and align the flexible optical elements.

Keywords: X-Ray Optics, Optical Alignment, Constellation-X, Spectroscopy X-Ray Telescope, Centroid Detector Assembly

1. INTRODUCTION

The Constellation-X Spectroscopy X-Ray Telescope (SXT) is one of the key components under development for the Constellation-X mission. The SXT optics assembly is a multi-shell, segmented X-ray mirror assembly which also provides an interface and mounting structure for the reflection grating assembly (RGA) portion of the reflection grating spectrometer, thermal pre and post-collimators and thermal control components. To demonstrate our readiness to build the SXT, we have put in place a phased development program in which all the elements of the SXT will be developed and tested. This program features a series of increasingly flight-like engineering development and prototype test units[1]. Broadly speaking, there are three major tasks involved in SXT development; optics and optic manufacturing, assembly and alignment and flight structure development. In this paper we address SXT development with a focus on assembly and alignment. In §2 we discuss SXT optical design, requirements and image error budget. In §3 we address assembly and alignment, including the evolution of the planned procedures, and in §4 we summarize our achievements to date.

X-Ray and Gamma-Ray Telescopes and Instruments for Astronomy, Joachim E. Trümper, Harvey D. Tananbaum, Editors, Proceedings of SPIE Vol. 4851 (2003)

2. SXT OPTICAL DESIGN, REQUIREMENTS AND ERROR BUDGET

2.1 Optical Design and Design Requirements

We have considered two grazing incidence design alternatives for the Constellation-X SXT: cone-cone and Wolter type 1. In each design the mirrors are densely packed. In the cone-cone design the mirrors are cylindrical cones. The Wolter 1 geometry is emulated by setting the secondary mirror slope angle to be three times larger than the primary mirror slope angle. A nested Wolter type 1 telescope consists of concentric grazing incidence parabolic (primary) and hyperbolic (secondary) mirrors. In the Wolter 1 design the slope angles of the secondary mirrors are set to be 3 times the slope angles of the primary mirrors at the primary/secondary intersection plane.

The cone-cone design lacks axial curvature the images from it are highly aberrated. This aberration alone would consume a large portion of our error budget and would force the tightening of other tolerances, such as manufacturing and alignment. A Wolter 1 design, however, forms a perfect on-axis image and was selected as the baseline design for the SXT. The Constellation-X SXT is a Wolter type 1 design with multiple segmented paraboloid/hyperboloid optics pairs. The angular extent of the smaller diameter segments will be a little less than 60 degrees and that of the larger diameter segments a little under 30 degrees (see Figure 4). A full P/H mirror shell will therefore be made up of either 12 (6P, 6H) or 24 (12P, 12H) individual segments, depending on radius. We are currently evaluating a range of options for shell axial length and number of shells. The choice will be made based on our development work. The axial length of each P or H element will range between 200mm and 300mm, the number of full optics shells between 230 and 167. We have selected this range based on mirror manufacturing, optical testing, mounting, alignment, and facility considerations. The nominal focal length will be 10,000mm and field of view at least 2.5 arc-minutes. The basic design dimensions and requirements for the CSX/SXT telescope are summarized in Table 1.

Parameter	Value
Axial distance from the primary-secondary intersection plane to telescope focus	10,000 mm
Primary and secondary mirror axial lengths	200mm – 300mm
Maximum reflector radius at the intersection plane	800 mm
Minimum reflector radius at the intersection plane	~150 mm
Axial distance from the back of the primary to the intersection plane	25.1 mm
Axial distance from the intersection plane to the front of the secondary	24.9 mm
Gap between the primary and secondary	50 mm
Mirror shell thickness	0.44 mm
Telescope field of view	2.5x 2.5 arc-minutes
Total mass per SXT (including 75 kgm for reflection grating assembly)	750 kgm
Mechanical Envelope	1700 mm D x 2060 mm L

Table 1 - Design dimensions and requirements for the CSX/SXT telescope

The baseline mirror thickness is 0.44 mm. This thickness includes the thickness of the glass sheet and the epoxy layer. The spacing between the primary and secondary is 50 mm. The primary-secondary intersection plane is moved 0.1mm towards the secondary mirror. This prevents any on-axis rays from missing the front edges of the secondary mirrors. The primary-secondary intersection planes of all the nested mirrors are located 10m from the focal plane of the telescope. The mirror shells are placed so that all the rays within the FOV pass the front and back edges of adjacent inner mirrors. The radial clearance for the extreme rays is 0.2 mm. This tolerance is added to prevent deformed or misaligned mirrors from obstructing the FOV. Under these assumptions up to 230 200-mm long mirror shells will fit between the minimum (~150 mm) and maximum (~800mm) radii. In case of 300-mm long mirrors, 167 shells can be placed in this radial range.

2.2 Effective Area

The top level mission requirement for effective area is 15,000 cm^2 at 1.25KeV and 6,000 cm^2 at 6.4KeV. This area is defined as the sum of the effective areas from both SXT instruments RGS and micro-calorimeter, taken at their respective focal planes (including all instrument effects) for all four satellites. We exclude from the area sum any areas for which the respective instrument does not meet the mission energy resolution requirements of 300 (min) and 3000 (above 6 keV). Since we will fly four identical satellites, each with a single SXT, we must split the throughput of the SXT between the RGS and Micro-Calorimeter. We apportion the SXT throughput by placing the reflective gratings over an outer annulus of the SXT, as shown in Figure 1. This is effective since the RGS is the primary low energy instrument and the outer mirrors, having larger graze angles, have most of their throughput at the lower energies. A ***preliminary*** allocation of the SXT area between the two instruments is shown in Table 2. This preliminary allocation allows us to meet our top level requirements, given current instrument performance characteristics.

2.3 Angular Resolution Requirement and System Level Error Budget

The angular resolution requirement for the SXT is 15 arc-seconds half-power diameter (HPD) over its 0.25 keV to 10 keV energy band. This is an on-orbit end-of-life requirement with all effects included. The telescope level spatial resolution error budget is shown in Figure 2. There are two major categories of contributors; telescope level effects and SXT optics on-orbit performance. Telescope level effects are those associated with the combined SXT optics/focal plane instrument combination. These effects include errors associated with reconstruction of the X-ray image, mounting of the SXT in the telescope, alignment and focus effects and on-orbit image smear due to vibration. The second major error category is "SXT Optics On-orbit Performance". This represents the performance of the SXT optics assembly only but in the on-orbit environment. Contributors to this category include impacts of launch, long term material stability, on-orbit thermally induced errors and, the largest sub-allocation, the SXT optics as-built on the ground. The "SXT Mirror, As-Built" category includes assembly strain, alignment errors and performance of the segmented optical elements. The largest single error allocation is for the optical elements[2] (~10 arcsec HPD). The allocation for assembly and alignment (~3 arcsec HPD) is small and challenging to meet. In this paper we describe the unique assembly and alignment approach which has been developed for Constellation-X and discuss its performance.

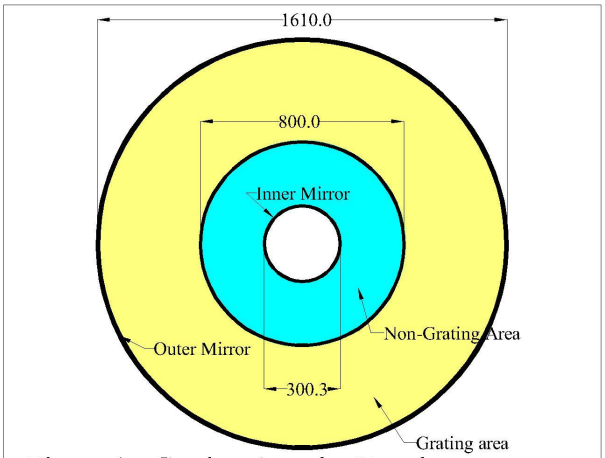

Figure 1 - Grating Annular Envelope

	Area per SXT (cm^2)		
E(keV)	**RGS**	**μCal**	**Total**
0.28	250	0	250
0.52	250	0	250
1.25	500	3250	3750
1.50	300	3450	3750
4.51	0	2000	2000
6.40	0	1500	1500
8.05	0	1000	1000
9.71	0	500	500

Table 2 – SXT Area Allocation to Instruments

SXT/Calorimeter Image Error Budget - Requirements								
ITEM (HPD - arcsec)	RQMT	Margin	Budget Allocation					
On-orbit Image Resolution	15.00	6.80	13.37					
Detector pixelization error (5 arcsec pixels)				4.08				
On-Orbit Telescope				12.73				
Telescope level effects					5.29			
Image Reconstruction errors (over obs)						4.24		
Attitude knowledge drift							3.00	
SXT/SI focal plane drift							3.00	
SXT/Telescope mounting strain						2.00		
SXT/SI vibration effects						2.00		
SXT/SI misalignment (off-axis error)						1.00		
SXT/SI Focus Error						1.00		
SXT Optics - On-orbit performance					11.58			
SXT Mirror launch shifts						2.00		
SXT thermally induced errors (ΔT driven)						3.61		
Housing/glass CTE mismatch							3.00	
Epoxy/glass bi-layer effects							2.00	
Long term material stability effects						1.00		
SXT Mirror, As-built						10.77		
Assembly (bonding) strain							3.00	
Alignment Errors (Using CDA)							3.00	
Optical Elements							9.90	

Figure 2 - SXT Angular Resolution Error Budget (yellow=requirement, red=RSS, green=allocation, magenta=margin)

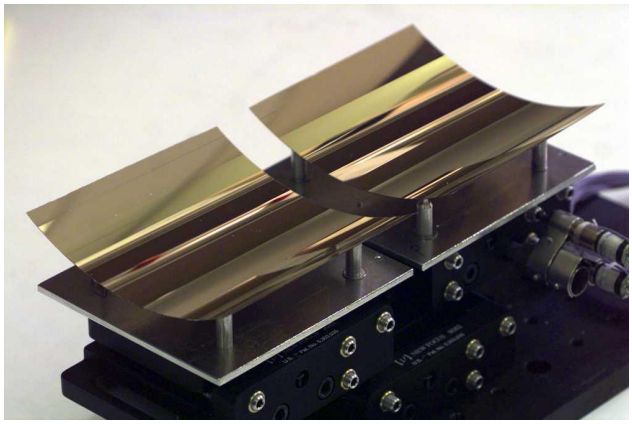

Figure 3 – Optical Segments

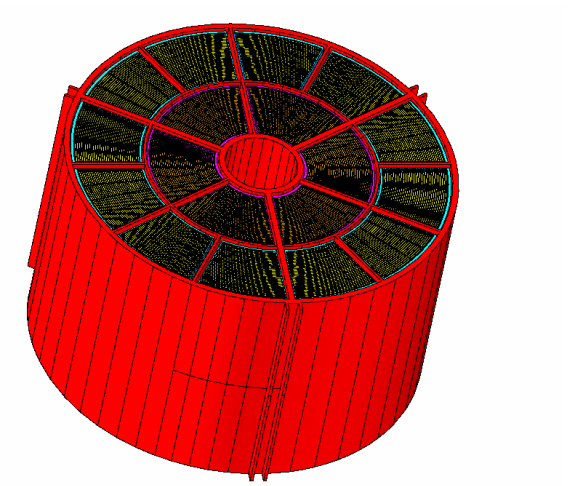

Figure 4 – SXT Modular Design

3. SXT ASSEMBLY AND ALIGNMENT

3.1 Segmented Optics Assembly and Alignment Overview

P and H optical segments, as shown in Figure 3, will be manufactured using the process described in Reference 2. After manufacture the segments will be assembled into wedge-shaped modules. Each module will contain from 50 to 150 optical segments, again depending on the final optical design. Each SXT, shown pictorially in Figure 4, will contain 36 total modules:

- 6 Paraboloid, Inner
- 6 Hyperboloid, Inner

- 12 Paraboloid, Outer
- 12 Hyperboloid, Outer

.

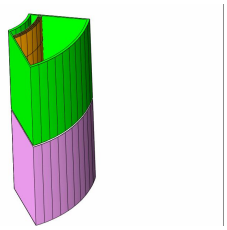

Figure 5 - Pictorial of P/H Module Pair with several optics installed

SXT alignment is performed first at the P/H module level, then the P/H module pairs are aligned with each other to form a complete SXT. A pictorial of a P/H module pair is shown in Figure 5. The alignment process is as follows:

- Within a P/H module pair:
  - Each H segment is aligned to its corresponding P segment, in 3 axes (axial, radial, and tangential) of position and rotation, according to the optical design, so that an X-ray image is formed at the desired telescope focus.
  - All P/H segment pairs within a P/H module pair are aligned to the common telescope focus.
- Module to module alignment:
  - The (6 or 12) P/H module pairs which comprise a complete (360° in azimuth) SXT are then aligned to each other so that the foci of all pairs are co-incident.

The alignment process for Wolter-I segmented optics is similar to that for full-shell optics in that the paraboloids and hyperboloids must be aligned to each other and in that all the multiple shells must be aligned so that they are confocal. However, for segmented optics there is an added requirement to align the segments of each full shell to each other so that they are also confocal. A P-H segment pair is shown in Figure 6. In it the traditional Wolter-I alignment errors; tilts, de-centers and defocus, are shown schematically. Figure 7 shows sensitivities to these types of rigid body errors for a 60 degree segmented P-H pair. Note that for the segmented optics the typical full shell focus and coma circles degenerate into 60° or 120° arcs.

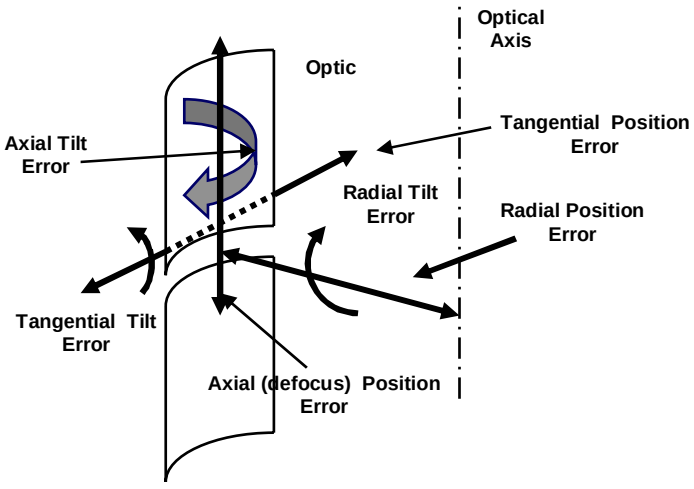

Figure 6 – Rigid Body Alignment Errors

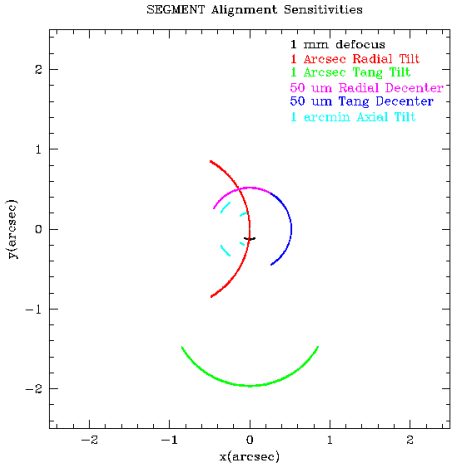

Figure 7 – Rigid Body Alignment Error Sensitivities

3.2 Assembly and Alignment of Segmented Optics

Design and production of the optical segments is described in detail in Reference 2. The as-manufactured segments are expected to have the following characteristics:

- Glass thickness between 400µm and 600µm.
- Epoxy thickness between 10µm and 40µm.
- Axial figure errors (2.3 arcsec RMS axial slope) and micro-roughness (5A°)
- Sag errors (±0.12 µm)
- Average radius errors within ±100µm
- Cone angle (Δ radius) errors within ±30 arc-seconds
- Circularity errors within ±10µm
- Errors at the ends of the segments, over a span of 5mm or less, of ± 5 µm

Several of the above optic characteristics have direct bearing on assembly and alignment, in particular, the presence of low-order axial and circularity errors of large magnitude as compared with the image requirements. ***This situation is typical for light-weight, flexible optics (Astro-E) and is dealt with in the assembly and alignment process by mechanically forcing the optics into the correct low-order shape (i.e., correct average radius, cone angle and circularity errors), as well as establishing the correct rigid body positioning for the optics. This has typically been done using the optic housing.*** These issues have been recognized and dealt with during the development of the Constellation-X SXT design, in particular in its assembly and alignment, as described below.

3.2.1 Error Budget Development – Mechanical Only Alignment Process and Tolerances

The system error budget shown in Figure 2 shows an allocation for assembly and alignment errors of only 3 arc-seconds (HPD). Our overall goal is to develop and demonstrate a process that meets this requirement and at the same time is practical for use in mass-production of SXT optics. The Constellation-X assembly and alignment process differs from that of previous missions with segmented optics in that the very lightweight, flexible optics must be aligned to much tighter tolerances to meet the image quality requirements. Our initial concept[3,4] for the alignment of the Constellation-X SXT was to rely exclusively on precision mechanical fixtures for the alignment. In this concept, an ultra-precision "reference cylinder" would be used to provide precise radii at various axial stations. Precision silicon etched "micro-combs" would be used as radial spacers to place the optics at their design radii, thereby both positioning the optical segments as required ***AND*** correcting for the low order errors as discussed above.

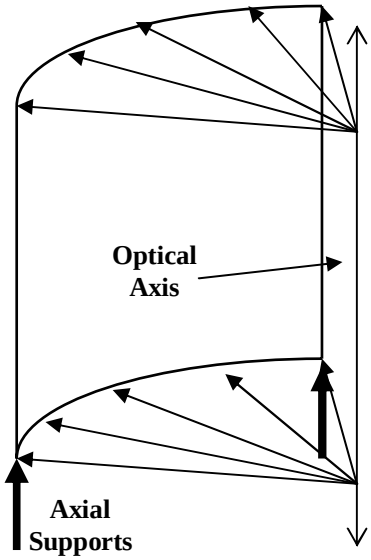

A schematic of the concept is shown in Figure 8, for one segment only. The optical axis of the telescope is shown as a vertical line. Ten radial position adjustment points are shown, five near the top edge and five near the bottom edge. The radial position of the segment will be forced into the correct radius at each of these 10 points. The reference cylinder and micro-comb setup are shown in Figure 9, also for one segment only.

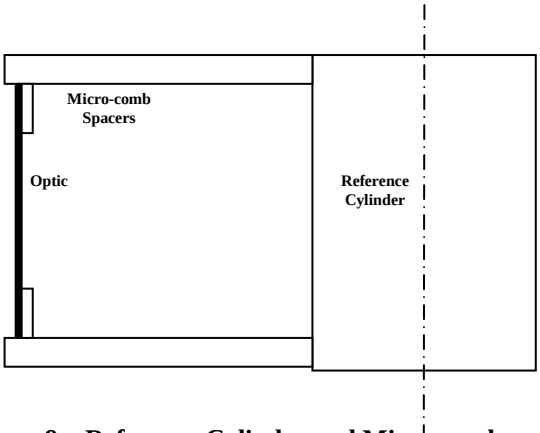

Figure 9 – Reference Cylinder and Micro-combs

An initial error budget, consistent with the 3 arc-second overall allocation to assembly/alignment, was developed for the mechanical alignment process. Two different types of errors were considered in the error budget process; 1) optic segment deformations and 2) optic segment rigid body errors. This was necessary since the alignment process, for flexible optics, establishes the low order axial figure as well as the optic rigid body position.

Optic Segment Deformations:

Average Radius error – We plan to force the radius into its design value. Any error in the average radius shifts the focus of the optic (or P-H pair). In the mechanical-only alignment process we would not shift the H mirror to adjust the pair focus (as in conventional X-ray optic alignment), so the errors due to this effect are limited by specification of mechanical tolerances. **(0.025 arcsec HPD per 1µm average radius error on P only**)

Delta Radius error – The difference in average radii of the 5 top radial positions from the 5 bottom positions. We plan to force delta radius to the design value. Errors in delta radius are cone angle errors, which offset the focus. Image quality is much more sensitive to delta radius errors than to average radius errors. **(4.1 arcsec HPD per 1µm delta radius error on P only)**

Random radial errors – Since we will force the radius of the segment (at ten positions) to conform to the radial positions of the assembly equipment, any variation in these radii produce deformations in the optic which degrade its performance. **(3.0 arcsec HPD for 1µm random radial errors, uniformly distributed, on both P and H)**

Rigid Body errors:

Axial position errors – During assembly, each segment is initially supported in two azimuthal positions. The average error in axial position from the ideal produces a defocus error (with very low sensitivity). The difference in axial positions (one to the other) produces a rotation about a radius through the center of the segment, which we have labeled "radial tilt error" (see Figure 5). **(0.26 arcsec HPD per 1mm axial position error between P and H; 1.0 arcsec HPD for 1arcsec radial tilt error on P only, caused by 1.1 µm axial position error between two supports)** A radial tilt error, however, can be largely corrected in the alignment process by deforming the optics so that the optical axis follows that defined by the mechanical reference.

Decenter errors – Rigid body position errors (normal to optical axis) between P and H segments. In two directions, aligned with the center radius of the segment (radial decenter) or tangent to the optic at its center (tangential decenter). Resulting image has coma. **(1.0 arcsec HPD per 50µm tangential or radial decenter)** These errors are controlled by the radial placement of the optic relative to the mechanical reference.

Tilt errors – Rigid body tilt of one segment relative to the other. Can be about either the center radius (see axial position errors above) or about a tangent to the optic at its center azimuth. **(3.8 arcsec HPD per 1 arcsec tangential tilt error)** These errors are also controlled by the radial placement of the optic relative to the mechanical reference.

Overall tolerances for radial errors at the alignment points are shown in Table 3. The mechanical fixtures must be designed to place the optic segment radii at their ***design values*** within these stated tolerances. These tolerances were established by a combination of finite element and raytrace analysis. Finite element models of P and H optical segments were developed. Ten cases were run for each optic (P and H), each case being a unit (1µm) displacement at one of the ten radial adjustment points, the other 9 being fixed. The

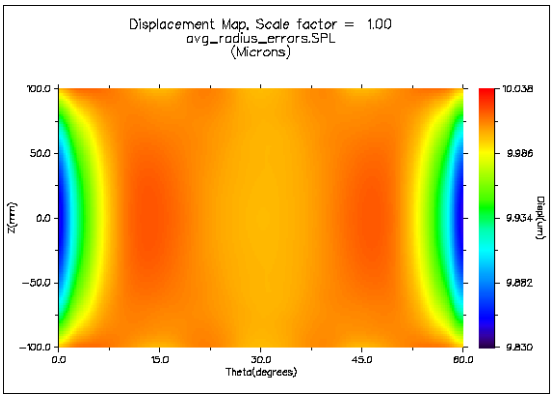

Figure 10 – Distortion Map, Average Radius Errors

effects of all 10 radial errors can be computed by multiplying the unit case distortions by the individual errors and summing the 10 distortion fields. Figure 10 shows a typical distortion map, in this case for 10µm radial errors at each point. It is interesting to note that even though the distortions at the 10 adjustment points are the same, the optic distortions are not uniform. This is due to the distortions being applied to a segment with edges, not a complete circular shell.

Error Term	Tolerance	At-Tolerance Performance Sensitivity Arc-seconds (HPD)	Prediction using Mechanical Alignment Only (Non-zero CTE)	Prediction using Mechanical Alignment Only (Zero-CTE)	Prediction using Opto-Mechanical Alignment
Average radius error:	10.0 µm	1	13.8 µm	10.7 µm	< 10.0 µm
Axial delta radius error	0.5 µm	2	5.6 µm	1.4 µm	< 0.5 µm
Random radial error	1.0 µm	3	2.8 µm	0.7 µm	< 1.0 µm
Radial tilt error	30 arcsec	0.2	29 arcsec	28.8 arcsec	< 30 arcsec

Table 3 – Mechanical Fixture Error Allocations

3.2.2 Achievement of Budgeted Tolerances

An initial assembly concept was developed based on the process described in references 3 and 4. This concept is illustrated in Figure 11. A precision reference cylinder provides radial positions at various axial stations. Spacers and precision "micro-combs" are used to radially position the optic (at 10 places) relative to the reference cylinder. In this concept, alignment of the optics depends on precise mechanical tolerances of the assembly fixturing; cylinder, spacers and micro-combs and on the optic figure at the ends. A mechanical tolerance analysis was performed on this design to estimate radial errors. This estimate is listed in Table 3 along with the required tolerance and performance impact. The table shows that none of the tolerances are met using the mechanical-only assembly approach. This is due to a number of factors. Although the silicon micro-combs may be manufactured to very high precision (well under 1µm accuracy), they are not long enough to span the space between the reference cylinder and the optic surface. We therefore require spacers between the reference cylinder and micro-combs. These spacers plus their installation add to the build-up of tolerances. The reference cylinder will be fabricated by diamond-turning. Both aluminum and titanium were considered as materials; lower CTE materials were not considered due to the difficulties in diamond-turning. The use of a non-zero CTE material, combined with the temperature control capability (±1°C) of the ***available*** assembly facilities, added large temperature-driven error terms. Finally, in addition to the mechanical fixture errors, the optics themselves can have radial errors at their ends as large as 5 µm. They can extend up to 5mm from the optic edge. Our radial adjustment points are approximately 2mm from the edge, so these end errors would add to the mechanical errors. Although many of these error sources might, in the long term, be reduced to within tolerance, we decided that we needed to explore alternate assembly techniques which would allow us to meet our immediate program goals for the OAP and, at the same time, provide potential for a better overall assembly process for the SXT.

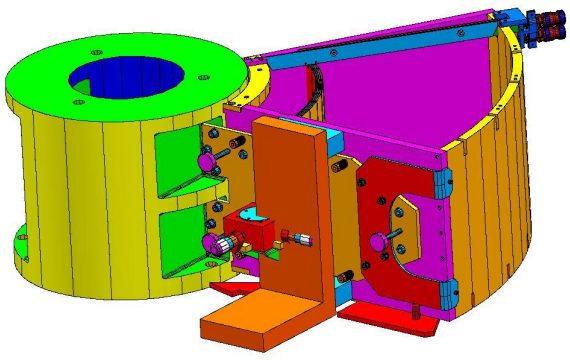

Figure 11 – Optic Housing and reference Cylinder

3.2.3 Revised Alignment Concept Using Fine Actuators and Optical Feedback

The conclusion of the initial error budget and mechanical tolerance work was that alignment of the SXT optics using mechanical means ***only*** was going to be very difficult to achieve. Even if the temperature effects were completely mitigated (see Table 3, "Zero CTE" column), the predicted radial errors would still be large enough to make the optical performance unacceptable. Given these results, we chose to investigate the use of optical alignment techniques, ***possibly in conjunction with precision mechanical fixtures***. We were familiar with the modified Hartmann alignment approach that had been successfully used to align the Chandra High Resolution Mirror Assembly to sub-arc-second tolerances[5] and undertook a study to determine if this technique could be adapted to Constellation-X.

Hartmann approaches in general work by testing small sub-apertures of a system to see where in the focal plane they cast an image. Any lateral errors in the location of the image indicate a corresponding wavefront slope error at the sub-aperture being tested. By testing many sub-apertures, these slope errors can be integrated to give total wavefront error. In a standard Hartmann approach, many sub-apertures, such as a ring of sub-apertures, are tested simultaneously, first slightly on one side of the focal plane, and then slightly on the other side. In the modified Hartmann approach used on Chandra, a pencil beam was sent from the nominal focal point of the telescope, through the telescope, to a retro-reflection flat, back through the telescope, and back again to the nominal focal point, where its lateral location was measured. This setup is shown in Figure 12. A specialized optical test set, the "Centroid Detector Assembly (CDA)", was developed by Bauer Associates, Inc. to implement this alignment procedure on Chandra. The CDA consists essentially of a laser source, beam steering optics to point the beam at various places in the annular aperture, a quadrant cell detector to sense the lateral location of the return beam, and beam splitting optics to separate the outgoing and return beams. The CDA is controlled from a PC computer via custom software. Fundamentally, the CDA produces the ***centroid location, in the focal plane*** for a selected Wolter optic (or P-H pair of optics) ***at a given azimuth angle within the annular X-ray aperture.*** For use in alignment, the CDA beam is scanned through a pre-defined set of azimuthal locations, stopping at each location and recording centroid data. These locations are fixed by the need for an aperture ***mask*** to stop the pencil beam down so that the return beam is only that reflected off the optic (or pair). The resulting set of data may then be analyzed to produce alignment information, traditionally focus, tilt and decenter.

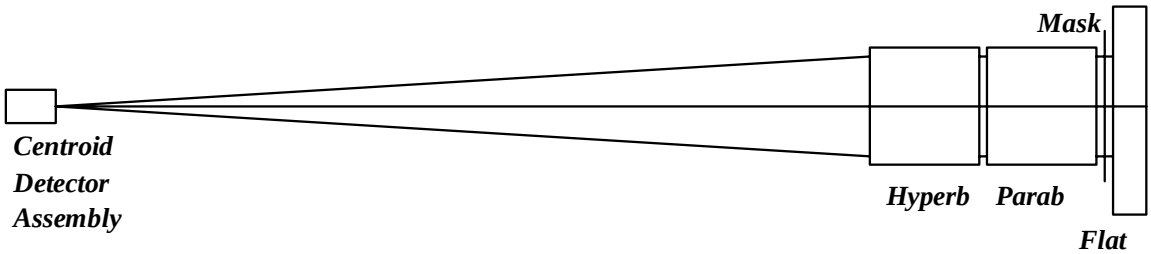

Figure 12 - Conceptual layout of the Centroid Detector Assembly in use aligning a mirror pair.

Adaptation of the CDA to Constellation-X segmented optics presented two issues:

- Would the CDA provide accurate centroid locations given the very narrow annular widths of the Constellation-X optics (diffraction issue?).
- Given good centroid data, how would it be used to align the optics?

The first issue was addressed by a Bauer study. Using optical analysis and modeling of the CDA, a simulation indicated that the centroids produced by the CDA would still be accurate to sub-arc-second levels, even including diffraction effects from the narrow apertures.

The second issue, use of CDA data for alignment, was less straightforward. Alignment of traditional, rigid full-shell Wolter-I optics using CDA data was a well-understood process. For the Constellation-X optics, however, alignment of 60 (or 30) degree shell segments was required. In addition, these segments are very flexible and, in fact, would not have the correct radii and cone angles per the optical design. Another issue was that designs were in place to assemble the optics mechanically, using micro-comb spacers and the reference cylinder, and it would help speed the process if

maximum use were made of existing designs and hardware. Over a period of several months, a revised alignment concept for the OAP unit was developed:

- The ten precision radial adjustment points (shown in Figures 8 and 9) were originally intended to be fixed at the design radii. In the new concept, manually driven precision mechanical adjusters would be used to adjust the radial positions of the optics at the ten locations.
- The CDA would be used to provide centroid data over the (nominal) 60 degree aperture and in particular at the five azimuths where the adjusters were located (average the data on each side of the adjuster, which blocks the CDA beam at the adjustment azimuth).
- The CDA data would be used in a "***point-by-point feedback mode***" to drive the adjustments so as to bring all of the centroids to the same location in the focal plane, thereby aligning the optics. The new idea in all of this is that the flexibility of the optics would be taken advantage of in the alignment process to provide five ***independent*** corrections, which could not be done if the optics were rigid. As an example, cone angle adjustments could be made by driving all actuators in or out by the same amount, thereby correcting the focus.

The hardware developed to perform these adjustments is shown in Figure 13 and discussed in Reference 6.

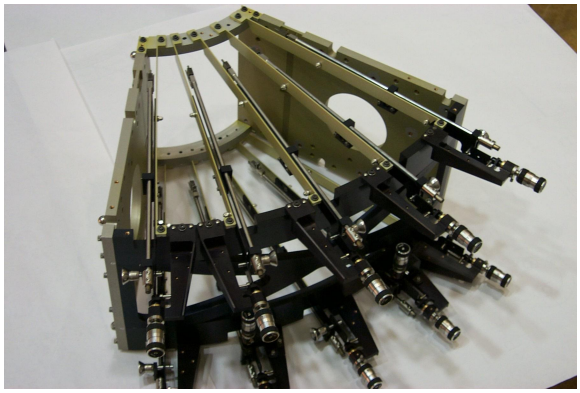

Figure 13 – OAP Adjustment Hardware

3.2.4 Analysis of Revised Alignment Concept

As described above, ten precision radial actuators (five top and five bottom) will be used to adjust the radial position of each optical segment (P and H). The Centroid Detector Assembly (CDA) will be used to measure the centroid of the image (in visible light) at a series of fixed azimuthal positions. The alignment process will simply be to use the radial actuators to drive all of the centroids to a single focused spot. This will be done initially for a P optic, then a P-H pair, followed by single P's and P-H pairs in the same module.

An example of the CDA driven alignment process is illustrated in Figure 14. The simulation is for a P-H pair with assumed optic errors and initial rigid body misalignments. Thirteen centroids are computed by a simulation of the CDA, roughly every 5 degrees over a 60 degree optic. In Figure 14 the centroid positions in the focal plane are plotted for the initial optic conditions and for five adjustments of the actuators. These adjustments are computed based on the centroid values ***at the five positions of the actuators*** and on the centroid adjustment scale factor of 2 arc-seconds of radial centroid shift per one µm adjuster motion. In the initial state the centroids are displaced by as much as 100 arc-seconds from the ideal focus, primarily due to a large cone angle error but with other errors (both rigid-body and non-rigid-body) as well. As adjustments are made the centroids collapse into nearly a single spot, with a consequent reduction in HPD.

Using this alignment process, we expect to largely correct for the following errors:

- **Optic Low Frequency Errors**: Circularity, Optic Average Radius, Optic cone angle, Roundness (partial), Delta-Delta-R (partial)
- **Initial Optic Position Errors:** Radial Position**,** Tangential position, **Axial** Position, **Radial** tilt, **Tangential** tilt (Derived from mechanical positioning tolerances for Radial Position, Axial Position and Tangential position).

A simulation of the alignment process has been performed to verify our ability to make the indicated corrections, in the presence of expected CDA centroiding errors. Inputs to the simulation were expected initial position errors, optic low frequency errors and CDA centroiding errors. Twenty cases were run, each with different error values, chosen randomly. In all cases the (simulated) alignment related errors fell below the budgeted 3 arc-second HPD.

3.2.5 In-process Interferometry

We will use normal incidence optical interferometry as a metrology tool on both the unmounted optics and mounted optics (during assembly and alignment). We will use a plane reference wavefront to test the axial figure error. For a conical part with no axial error, correctly aligning this wavefront to the part will return a good null error wavefront. As only at one azimuth is the beam normal to the part, we only get profiles using this method. Figure 15 shows this test geometry, using a 6" expanded beam on a mandrel; the same test works for either mandrels or optics. We use a custom built 20cm beam expander for the OAP optic axial lengths.

Figure 14 - CDA Alignment Example

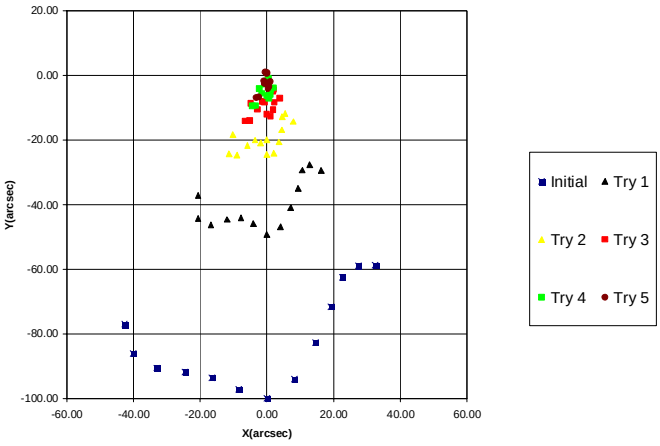

As our parts are true Wolter-I parts, there is a slight wavefront error (~2.8 µm P/V for these parts) due to the Wolter axial sag as compared to a best-fit cone. For our purposes, higher order terms beyond curvature are negligible. First, the formed glass substrates are tested. As the forming mandrels are conical, we compare these parts to the best fit cone and screen the substrates to select the best ones for replication. The fully replicated foils are compared to the nominal Wolter curvature (slightly different for the primary and secondary) to assess the axial figure errors unmounted.

We have also planned for in-situ testing using the same equipment, using steerable fold flats (5x23 cm) to bring the beam to the mounted optic in normal incidence to repeat this axial figure measurement. This will test the difference in mounted vs. unmounted axial figure error, and, in conjunction with the CDA, should allow the separation of figure from alignment errors. However, once we move beyond a single pair of foils, we will have access only to the innermost pair of foils.

A second test geometry, using a fast (f/0.75) reference lens, allows testing of azimuthal figure error, as shown in Figure 16. Again, only profiles are returned, and again this test is used on unmounted mirrors to screen substrates and to test replicated foils before mounting. As used in-situ, this test has a significantly larger range of depths at which fringes can be seen in the interferometer video monitor than can be measured. However, this affords a means of getting from mechanical levels of azimuthal (circularity) alignment to the optical level. Once aligned for optical testing, the azimuthal profile can be used to dictate which azimuthal adjustments are made. To view different axial locations on the mirror, the interferometer will be moved vertically.

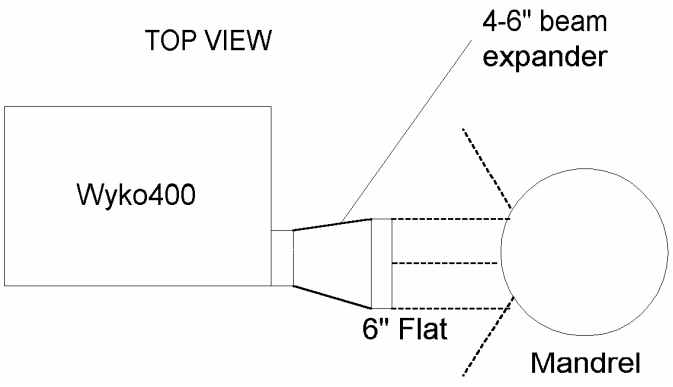

Figure 15 – Axial Figure Metrology

4. SUMMARY

We have established a phased program to demonstrate technical readiness for manufacture of the Constellation-X SXT. Analysis has led us to revise our assembly approach from a purely mechanical one to one which makes optimal use of optical feedback, and have adapted the Chandra

CDA for use in SXT assembly and alignment. Analysis indicates that, using the modified approach, we can meet the alignment error budget allocation for the 15 arc-second (HPD) SXT requirement. We plan to demonstrate this by test in the next several months.

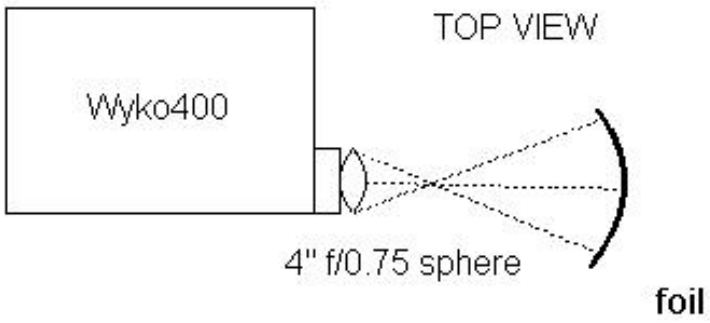

Figure 16 – Azimuthal Figure Metrology

After we demonstrate the alignment of a single pair of optics to requirements we plan to address two other issues; environmental sensitivity and assembly of multiple segments within a module. Preliminary analysis has indicated that the module housing must be well matched with the glass, in terms of CTE, so as to avoid image degradation as the temperature moves off-nominal. In test units subsequent to the OAP we plan to use materials with better matched better CTE's. Assembly of multiple segments will be addressed by combining the use of precision mechanical fixtures (micro-combs), optical feedback from the CDA and automated alignment actuators. Mass production techniques are now being explored.

In summary, we believe that out development and test program will demonstrate our readiness to build the SXT in support of the Constellation-X program schedule.

5. ACKNOWLEDGEMENTS

This work was supported by NASA Goddard Co-operative agreement NCC5-368.

6. REFERENCES

1. R. Petre, W. W. Zhang, D. A. Content, T. T. Saha, J. Stewart, J. H. Hair, D. Nguyen, W. A. Podgorski, W. R. Davis, Jr., M. D. Freeman, L. M. Cohen, M. L. Schattenburg, R. K. Heilmann, Y. Sun, C. Forest, "Constellation-X spectroscopy x-ray telescope (SXT)", SPIE 4851-50
2. W. W. Zhang, K. Chan, D. A. Content, R. Petre, P. J. Serlemitsos, T. T. Saha, Y. Soong, "Development of mirror segments for the Constellation-X observatory", SPIE 4851-58
3. G. P. Monnelly, D. Breslau, N. Butler, C. G. Chen, L. M. Cohen, W. Gu, R. K. Heilmann, P. T. Konkola, O. Mongrard, G. R. Ricker Jr., and M. L. Schattenburg , "High-Accuracy X-Ray Foil Optic Assembly", Proc. SPIE 4138, 164 (2000).
4. C. G. Chen, L. M. Cohen, R. K. Heilmann, P. T. Konkola, O. Mongrard, G. P. Monnelly, and M. L. Schattenburg, "Micro-Comb Design and Fabrication for High-Accuracy Optical Assembly", J. Vac. Sci. Technol. B 18, 3272 (2000).
5. P. E. Glenn, "Centroid detector assembly for the AXAF-I alignment test system", SPIE 2515, pp352-360 (1995)
6. Hair, J. Stewart, R. Petre, W. W. Zhang, D. A. Content, T. T. Saha, W. A. Podgorski, P. E. Glenn, M. L. Schattenburg, R. K. Heilmann, Y. Sun, G. Nanan, "Constellation-X soft x-ray telescope segmented optic assembly and alignment implementation", SPIE 4851-76